Observation of multiple hard photon final states at $\sqrt{s} =$ 130-140 GeV at LEP

M. Acciarri, A. Adam, O. Adriani, M. Aguilar-Benitez, S. Ahlen, B. Alpat, J. Alcaraz, G. Alemanni, J. Allaby, A. Aloisio, et al.

EUROPEAN ORGANIZATION FOR NUCLEAR RESEARCH

CERN-PPE/96-48
March 28, 1996

Observation of multiple hard photon final states at $\sqrt{s} = 130 - 140$ GeV at LEP

The L3 Collaboration

Abstract

We have studied the process $e^+e^- \to n\gamma$ ($n \geq 2$) at an average center-of-mass energy of 133 GeV using the L3 detector at LEP. For an integrated luminosity of 4.95 pb^{-1} we find one $\gamma\gamma\gamma\gamma(\gamma)$ final state with only hard photons. The rates of both $\gamma\gamma\gamma$ and $\gamma\gamma$ events are consistent with QED expectations. The cross section of the reaction $e^+e^- \to \gamma\gamma(\gamma)$ in the polar range $16^\circ < \theta_\gamma < 164^\circ$ is measured to be 22.6 $\pm$ 2.2 pb. Decays into photons of narrow scalar resonances with masses between 90 and 130 GeV are not observed. The observation of the event with four energetic photons is consistent with QED although the kinematic configuration of the photons is atypical.

Submitted to *Phys. Lett. B*

Introduction

The reaction $e^+e^- \to n\gamma$ ($n \geq 2$) is well suited to test QED in the vicinity of the Z resonance since the expected contribution from the weak sector of the Standard Model is extremely small [1]. The reaction $e^+e^- \to n\gamma$ ($n \geq 3$) is also a potential source of new physics, especially at high energies [2,3]. Above the Z resonance, channels not involving direct Z production become interesting [4,5] and easier to detect. We present a detailed analysis of these processes using the data collected with the L3 detector during the 1995 high-energy run at $\sqrt{s} = 130 - 140$ GeV.

The potential of the process $e^+e^- \to \gamma\gamma(\gamma)$ for probing possible QED deviations increases with luminosity and energy. At center-of-mass energies in the range 130-140 GeV, and for an integrated luminosity of 5 pb^{-1}, the sensitivity becomes similar to the one already reached at LEP1 with an order of magnitude more integrated luminosity [6,7].

The L3 Detector

The L3 detector is described in detail in Ref. [8] The main components of the detector relevant to the analysis are the central tracking chamber (TEC), a high-resolution electromagnetic calorimeter (ECAL) composed of bismuth germanium oxide (BGO) crystals with a barrel region ($42^\circ < \theta < 138^\circ$) and two endcaps ($11^\circ < \theta < 37^\circ$ and $143^\circ < \theta < 169^\circ$), a ring of scintillation counters, a sampling hadron calorimeter (HCAL) with uranium absorbers and proportional wire chamber readout, and a high precision muon spectrometer. Forward BGO arrays on either side of the detector measure the luminosity by detecting small-angle Bhabha events. All subdetectors are located in a 12 m diameter magnet which provides a uniform field of 0.5 T along the beam direction. The energy and angular resolution for electrons and photons with energies above 1 GeV are better than 2% and 0.5°, respectively.

Event Selection

The following cuts have been applied to select events with two or more photons:

(1) The number of photon candidates in the range of polar angles $16^\circ < \theta_\gamma < 164^\circ$ must be at least two. A photon candidate is:

- a shower in the ECAL with energy above 1 GeV and a profile consistent with that of an electron or a photon, or
- a cluster in the first 22 radiation lengths of the hadron calorimeter in the angular region $0.74 <| \cos\theta_\gamma |< 0.80$, where there is no ECAL coverage.

(2) The number of TEC signals found along the path of any photon candidate must be less than 40% of the total expected for a charged particle.

(3) The total electromagnetic energy must be greater than $0.5\sqrt{s}$.

The sample analysed corresponds to a total integrated luminosity of 4.95 pb^{-1}, shared as follows: 2.64 pb^{-1} at $\sqrt{s} = 130$ GeV, 2.26 pb^{-1} at $\sqrt{s} = 136$ GeV and 0.05 pb^{-1} at $\sqrt{s} = 140$ GeV. The average center-of-mass energy is 133 GeV. After all cuts have been applied, 107 $e^+e^- \to n\gamma$ ($n \geq 2$) events are selected. The contamination from Bhabha events is negligible. All candidates have been visually scanned.

The selected events are classified according to the number of observed isolated photons. An isolated photon must form an angle greater than 15° with any other photon in the event. The sample is composed of 102 events with two photons, 4 events with three photons and 1 event with four photons.

In order to determine the acceptance of the selection cuts the same analysis has been applied to a sample of events from a QED Monte Carlo generator [9]. This generator includes soft and hard bremsstrahlung, and virtual-photon corrections up to $O(\alpha^3)$. The generated events are passed through the L3 simulation and reconstruction programs. The overall efficiency for selecting events with the two most energetic photons in the range $16^\circ < \theta_\gamma < 164^\circ$ is found to be $(95.0 \pm 0.3)\%$, rather uniform down to the acceptance limit. The trigger efficiency is estimated to be 99.7%.

$\gamma\gamma\gamma\gamma(\gamma)$ events

We have found one event with four energetic photons (Figure 1). The energies and directions of the photons are given in Table 1. The least energetic one has 7 GeV and the lowest polar angle is $\cos\theta_\gamma = -0.9$. The visible energy of the event is $E_{vis} = 90.0 \pm 0.7$ GeV and the missing energy is $E_{miss} = 40.3 \pm 0.7$ GeV. The invariant mass of the 4-photon system is $M_{4\gamma} = 80.0 \pm 0.8$ GeV. It is balanced in the transverse plane ($p_x = 0.1 \pm 0.6$ GeV, $p_y = -0.1 \pm 1.0$ GeV) and the longitudinal missing momentum is $p_{||} = 41.2 \pm 1.3$ GeV, in agreement with the hypothesis of a missing zero-mass particle. Therefore, the event is consistent with a QED process $e^+e^- \to \gamma\gamma\gamma\gamma\gamma$, where one of the photons escapes detection at very low polar angle.

$\sqrt{s}$ (GeV)	Photon energy (GeV)	θ_γ (deg)	ϕ_γ (deg)
130.3	50.1	154.7	301.6
	19.8	57.4	114.7
	13.2	112.5	149.2
	7.0	102.8	333.4

Table 1: Event with four photons at a center-of-mass energy of 130 GeV. The resolution on the photon energy measured in the ECAL is better than 2% for all cases. The angular resolution ($\Delta\phi_\gamma \simeq 1$ mrad, $\Delta\theta_\gamma \simeq 20$ mrad) is dominated by the uncertainty in the position of the event vertex along the beam axis.

The presence of an energetic photon at very low polar angle is not unusual. In the $e^+e^- \to \gamma\gamma(\gamma)$ process, $O(\alpha^3)$ corrections [9] give a very small contribution to the tree-level cross section when fiducial cuts have been applied. The amount of collinear radiation [1)] is however not negligible. In Figure 2 the experimental spectrum of the energy of collinear photons in $\gamma\gamma(\gamma)$ events is shown, compared with the Monte Carlo prediction. Almost 25% of the events have photon emission above 8 GeV. The same kind of behavior is expected with four visible photons.

Multiphoton production at high energies has also been observed at LEP1. We have analysed recent LEP1 data with the same experimental cuts as used above. For an integrated luminosity of 63.7 pb^{-1}, we find 4 $\gamma\gamma\gamma\gamma(\gamma)$ candidates. The one with the most energetic collinear photon

[1)] By collinear radiation we mean photon emission extremely close to the beam particles.

is shown in Figure 3 and Table 2. It is consistent with a collinear photon of 27 GeV. For all candidates the least energetic photon has an energy between 1 and 2 GeV.

$\sqrt{s}$ (GeV)	Photon energy (GeV)	θ_γ (deg)	ϕ_γ (deg)
89.5	34.1	31.6	328.6
	19.2	113.0	140.3
	7.3	20.0	220.3
	1.56	158.9	315.0

Table 2: Event with four photons at a center-of-mass energy of 89 GeV. The resolution on the photon energy measured in the ECAL is better than 2% for all cases. The angular resolution ($\Delta\phi_\gamma \simeq 1$ mrad, $\Delta\theta_\gamma \simeq 20$ mrad) is dominated by the uncertainty in the position of the event vertex along the beam axis.

In order to compare the data with the QED predictions we have used the matrix element computed in [10] and written a Monte Carlo generator of the process $e^+e^- \to \gamma\gamma\gamma\gamma$ at the tree level. Energy and angular cuts have been implemented and reference [11] has been used for the phase space generation. The cross sections from this generator have been compared with those obtained using a different program [12]. They are found to be in agreement within the statistical uncertainty (± 1 fb). We estimate a visible cross section at $\sqrt{s} = 133$ GeV of 40 fb, which corresponds to 0.2 events expected in the total sample. The prediction at LEP1 is 70 fb, which corresponds to 4.5 events expected. The data are in good agreement with the predictions.

The Monte Carlo spectrum of the least energetic photon in $\gamma\gamma\gamma\gamma$ events at $\sqrt{s} = 133$ GeV is shown in Figure 4. It is strongly peaked at low energies. Only 20% of the events have all photons with an energy above 7 GeV. As for the $\gamma\gamma(\gamma)$ sample, $O(\alpha^5)$ corrections are not expected to modify significantly the tree level $\gamma\gamma\gamma\gamma$ cross section in the fiducial volume. The effect of hard photon radiation has been simulated assuming in an uncorrelated way the same collinear spectrum of the $\gamma\gamma(\gamma)$ Monte Carlo generator [2]. We estimate a probability of 0.5 % for finding a $\gamma\gamma\gamma\gamma(\gamma)$ event in a 5 pb^{-1} sample at $\sqrt{s} = 133$ GeV in which the energy of all visible photons is above 7 GeV and the energy of an additional collinear photon is above 40 GeV.

We conclude that the observation of this event is consistent with QED although the kinematic configuration of the photons is atypical.

$\gamma\gamma\gamma(\gamma)$ events and search for compositeness

The number of $e^+e^- \to \gamma\gamma\gamma$ events with three observed isolated photons is estimated to be 5.8 from the Monte Carlo simulation. We find four events. All of them have a planar configuration and no significant missing energy-momentum. The observed rate and the event characteristics are in agreement with QED.

Production of rare decays like $Z \to \gamma\gamma\gamma$ is not favored at energies above the Z peak. However, limits can be set on forbidden processes like $e^+e^- \to (\gamma, Z)^* \to S\gamma$, where S is a narrow scalar resonance with $ZS\gamma$ and $S\gamma\gamma$ couplings and decaying mainly into photon pairs. Such a process

[2] After cuts, the collinear photon emission is expected to be decoupled from the kinematic properties of the visible photons to a good approximation. This assumption has been checked to be valid in the case of the $\gamma\gamma$ process, for which the exact $O(\alpha^3)$ generator [9] is available.

is expected in the context of compositeness models [2, 4, 5]. We have simulated the signal with different hypotheses for the coupling constants [5], taking also into account initial-state corrections [13]. The acceptance is 83-85% for S masses in the range 90-130 GeV. The highest $\gamma\gamma$ invariant masses found in the four $\gamma\gamma\gamma$ events are 117, 124, 129 and 134 GeV. The expected invariant mass resolution is 1 GeV. We exclude at the 95% confidence level (CL) Born level cross sections above 0.9 pb for invariant masses up to 115 GeV and above 1.4 pb for the whole 90-130 GeV range.

Events with two visible photons and longitudinal missing energy can be used to search for the process $e^+e^- \to \gamma S$; $S \to \gamma\gamma$, S being the scalar resonance introduced before, but now also allowed to couple to electrons [4]. The good resolution of the L3 detector permits the identification of narrow width resonances at these energies. We have compared QED and data for the invariant masses of the two observed photons (Figure 5). No significant deviations are observed. We set upper limits (at the 95% CL) on the product of branching ratios $B_{ee}B_{\gamma\gamma}$, where B_{ee} is the branching ratio of the scalar resonance into electron pairs and $B_{\gamma\gamma}$ is its branching ratio into photon pairs. The limits are shown in Figure 5. They are in the range $0.01 - 0.05$, depending on the mass and width of the resonance.

Limits on QED deviations from the $\gamma\gamma(\gamma)$ sample

Figure 6 shows the differential cross section as a function of $\cos\theta$ [3] , compared with the Monte Carlo distribution. Good agreement is observed. We measure the cross section for $e^+e^- \to \gamma\gamma(\gamma)$ with the two most energetic photons in the range $16^\circ < \theta_\gamma < 164^\circ$ to be 22.6 ± 2.2 pb, where the error is purely statistical. Systematic effects have been found to be much smaller than the statistical error and are neglected. The result is also in good agreement with the QED expectation of 22.2 pb at $\sqrt{s} = 133$ GeV. The acollinearity distribution of the two most energetic photons is shown in Figure 7. The data follow the QED predictions.

We look for deviations from QED following the general approach suggested in Ref. [14]. This approach makes use of effective interactions with non-standard $e^+e^-\gamma$ couplings and $e^+e^-\gamma\gamma$ contact terms. Independently of the type of deviation under consideration, only two forms are relevant depending on the center-of-mass energy and the polar angle:

$$\frac{d\sigma}{d\Omega} = \left(\frac{d\sigma}{d\Omega}\right)_{\rm QED}\left(1 + \frac{s^2}{\alpha}\frac{1}{\Lambda^4}\left(1-\cos^2\theta\right)\right) \quad (1)$$

$$\frac{d\sigma}{d\Omega} = \left(\frac{d\sigma}{d\Omega}\right)_{\rm QED}\left(1 + \frac{s^3}{32\pi\alpha^2}\frac{1}{\Lambda'^6}\frac{\left(1-\cos^2\theta\right)}{\left(1+\cos^2\theta\right)}\right) \quad (2)$$

where Λ, Λ' are free parameters with dimensions of energy. Limits on the contact interaction scale parameter Λ have been already set in our previous publication [6]. The sensitivity on Λ' increases rapidly with the center-of-mass energy, making these new energies advantageous with respect to LEP1.

A simple and convenient way of parametrizing the deviations from QED is also the introduction of cut-off parameters $\Lambda_\pm$ [15, 16]. They can be treated in practice as one of the types above, using $\Lambda^4 = \pm(2/\alpha)\Lambda_\pm^4$. Another way is to postulate the existence of an excited electron,

[3] We define the polar angle of the event as $\cos\theta = \left|\ \sin(\frac{\theta_1-\theta_2}{2})/\sin(\frac{\theta_1+\theta_2}{2})\ \right|$, where θ_1 and θ_2 are the polar angles of the two most energetic photons in the event. The angle θ is the polar angle in the center-of-mass system of the two photons under the assumption of an additional undetected photon along the beam direction.

e^*, with mass m_{e^*}. Such a particle can couple to the electron and the photon via magnetic interactions. The complete expression for the differential cross section as a function of m_{e^*}, the center-of-mass energy and its coupling strength, λ, can be found in [16]. We will assume this coupling constant to be 1.

In order to quantify the deviations from QED, we have performed maximum likelihood fits for the Λ, Λ' and m_{e^*} hypotheses:

$$L(\mathrm{T_p}) = \frac{1}{\sqrt{2\pi}\sigma(\mathrm{T_p})} \exp\left(\frac{-(N_o - N_t(\mathrm{T_p}))^2}{2\sigma^2(\mathrm{T_p})}\right) \prod_{i=1}^{N_o} P(\cos\theta_i; \mathrm{T_p}) \tag{3}$$

where $\mathrm{T_p}$ stands for the parameter $1/\Lambda^4$, $1/\Lambda'^6$ or $1/m_{e^*}^4$. This choice of parameters has the advantage of giving fitted values with almost symmetric Gaussian errors. N_o is the total number of observed events; $N_t(\mathrm{T_p})$ is the total number of expected events and $P(\theta_i; \mathrm{T_p})$ is the event probability density, taking into account the exact functional shapes and efficiencies as a function of $\cos\theta$. The error $\sigma(\mathrm{T_p})$ is the statistical error on the number of expected events.

The results of the fits are the following:

$$\frac{1}{\Lambda^4} = \left(+0.36^{+\ 0.45}_{-\ 0.41}\right)\ 10^{-11}\ \mathrm{GeV}^{-4} \tag{4}$$

$$\frac{1}{\Lambda'^6} = \left(+1.93^{+\ 2.24}_{-\ 2.00}\right)\ 10^{-16}\ \mathrm{GeV}^{-6} \tag{5}$$

$$\frac{1}{m_{e^*}^4} = \left(+1.13^{+\ 1.30}_{-\ 1.15}\right)\ 10^{-9}\ \mathrm{GeV}^{-4} \tag{6}$$

All values are consistent with no deviation from QED. To determine the confidence levels, the probability distribution is normalized over the physically allowed range for the parameters, as suggested in [17]. At the 95% CL we obtain:

$$\Lambda > 535\ \mathrm{GeV} \tag{7}$$

$$\Lambda' > 342\ \mathrm{GeV} \tag{8}$$

$$\Lambda_+ > 131\ \mathrm{GeV} \tag{9}$$

$$\Lambda_- > 167\ \mathrm{GeV} \tag{10}$$

$$m_{e^*} > 129\ \mathrm{GeV} \tag{11}$$

Conclusions

We have studied the reaction $e^+e^- \to n\gamma$ ($n \geq 2$) at an average center-of-mass energy of $\sqrt{s} = 133$ GeV. The measurements of the total and differential cross sections for $e^+e^- \to \gamma\gamma(\gamma)$ are well described by QED. Using only data at $\sqrt{s} = 133$ GeV, we set the following lower limits at the 95% confidence level: the contact interaction energy scale parameters $\Lambda > 535$ GeV and $\Lambda' > 342$ GeV; the QED cut-off parameters $\Lambda_+ > 131$ GeV and $\Lambda_- > 167$ GeV; and the excited electron mass $m_{e^*} > 129$ GeV.

We observe 4 events with three photons seen in the detector, in agreement with a QED expectation of 5.8 events. No evidence of composite narrow scalar resonances decaying into photons has been found in the energy range 90-130 GeV. We observe one $e^+e^- \to \gamma\gamma\gamma(\gamma)$ event with high energy photons. The observation of this event is consistent with QED although the kinematic configuration of the photons is atypical.

Acknowledgements

We wish to express our gratitude to the CERN accelerator divisions for the excellent performance of the LEP machine. We acknowledge the effort of all engineers and technicians who have participated in the construction and maintenance of the experiment. We also thank T.Kaneko for the computation of cross sections using the GRACE program.

References

[1] E.W.N. Glover and A.G. Morgan, Z. Phys. **C 60** (1993) 175.

[2] F. Boudjema and F. Renard, in "Z Physics at LEP 1", eds. G. Altarelli *et al.*, CERN Report 89-08 vol. 2, p. 185;
M. Baillargeon and F. Boudjema, in "Workshop on Photon Radiation from Quarks", CERN Report 92-04, ed. S. Cartwright, (1992) p. 178.

[3] A. De Rújula, Nucl. Phys. B435 (1995) 257.

[4] M. Renard, Z. Phys. **C24** (1984) 385.

[5] M. Renard, Phys. Lett. **B126** (1983) 59.

[6] L3 Collab., M. Acciarri *et al.*, Phys. Lett. **B 353** (1995) 136.

[7] OPAL Collab, M.Z. Akrawy *et al.*, Phys. Lett. **B 257** (1991) 531.
ALEPH Collab., D. Buskulic *et al.*, Z. Phys. **C 59** (1993) 215.
DELPHI Collab., P. Abreu *et al.*, Phys. Lett. **B 327** (1994) 386.

[8] L3 Collab., B. Adeva *et al.*, Nucl. Inst. Meth. **A 289** (1990) 35.
L3 Collab., O. Adriani *et al.*, Physics Reports **236** (1993) 1.

[9] F.A. Berends and R. Kleiss, Nucl. Phys. **B 186** (1981) 22.

[10] CALKUL Collaboration, F.A. Berends *et al.* , Nucl. Phys. **B239** (1984) 395.

[11] R. Kleiss, W. J. Stirling and S. D. Ellis , Comp. Phys. Comm. **40** 1986 359.

[12] MINAMI-TATEYA Group, GRACE Manual, KEK Report 92-19.

[13] F.A. Berends and R. Kleiss, Nucl. Phys. **B 260** (1985) 32.

[14] O. J. P. Eboli *et al.*, Phys. Lett. **B271** (1991) 274.

[15] F.E. Low, Phys. Rev. Lett. **14** (1965) 238;
R. P. Feynman, Phys. Rev. Lett. **74** (1948) 939;
F. M. Renard, Phys. Lett. **B116** (1982) 264;
S. Drell, Ann. Phys. (N.Y.) **4** (1958) 75.

[16] A. Litke, Harvard Univ., Ph.D Thesis (1970) unpublished.

[17] Particle Data Group, Phys. Rev. **D 50** (1994) 1278.

The L3 Collaboration:

M.Acciarri,[29] A.Adam,[48] O.Adriani,[18] M.Aguilar-Benitez,[28] S.Ahlen,[12] B.Alpat,[36] J.Alcaraz,[28] G.Alemanni,[24] J.Allaby,[19] A.Aloisio,[31] G.Alverson,[13] M.G.Alviggi,[31] G.Ambrosi,[36] H.Anderhub,[51] V.P.Andreev,[40] T.Angelescu,[14] D.Antreasyan,[10] A.Arefiev,[30] T.Azemoon,[3] T.Aziz,[11] P.Bagnaia,[39] L.Baksay,[46] R.C.Ball,[3] S.Banerjee,[11] K.Banicz,[48] R.Barillère,[19] L.Barone,[39] P.Bartalini,[36] A.Baschirotto,[29] M.Basile,[10] R.Battiston,[36] A.Bay,[24] F.Becattini,[18] U.Becker,[17] F.Behner,[51] J.Berdugo,[28] P.Berges,[17] B.Bertucci,[19] B.L.Betev,[51] M.Biasini,[19] A.Biland,[51] G.M.Bilei[36] J.J.Blaising,[19] S.C.Blyth,[37] G.J.Bobbink,[2] R.Bock,[1] A.Böhm,[1] B.Borgia,[39] A.Boucham,[4] D.Bourilkov,[51] M.Bourquin,[21] E.Brambilla,[17] J.G.Branson,[42] V.Brigljevic,[51] I.C.Brock,[37] A.Buijs,[47] A.Bujak,[48] J.D.Burger,[17] W.J.Burger,[21] J.Busenitz,[46] A.Buytenhuijs,[33] X.D.Cai,[20] M.Campanelli,[51] M.Capell,[17] G.Cara Romeo,[10] M.Caria,[36] G.Carlino,[4] A.M.Cartacci,[18] J.Casaus,[28] G.Castellini,[18] R.Castello,[29] F.Cavallari,[39] N.Cavallo,[31] C.Cecchi,[21] M.Cerrada,[28] F.Cesaroni,[25] M.Chamizo,[28] A.Chan,[53] Y.H.Chang,[53] U.K.Chaturvedi,[20] M.Chemarin,[27] A.Chen,[53] G.Chen,[8] G.M.Chen,[8] H.F.Chen,[22] H.S.Chen,[8] X.Chereau,[4] G.Chiefari,[31] C.Y.Chien,[5] M.T.Choi,[45] L.Cifarelli,[41] F.Cindolo,[10] C.Civinini,[18] I.Clare,[17] R.Clare,[17] H.O.Cohn,[34] G.Coignet,[4] A.P.Colijn,[2] N.Colino,[28] V.Commichau,[1] S.Costantini,[39] F.Cotorobai,[14] B.de la Cruz,[28] T.S.Dai,[17] R.D'Alessandro,[18] R.de Asmundis,[31] H.De Boeck,[33] A.Degré,[4] K.Deiters,[49] P.Denes,[38] F.DeNotaristefani,[39] D.DiBitonto,[46] M.Diemoz,[39] D.van Dierendonck,[2] F.Di Lodovico,[51] C.Dionisi,[39] M.Dittmar,[51] A.Dominguez,[42] A.Doria,[31] I.Dorne,[4] M.T.Dova,[20,♯] E.Drago,[31] D.Duchesneau,[4] P.Duinker,[2] I.Duran,[43] S.Dutta,[11] S.Easo,[36] Yu.Efremenko,[34] H.El Mamouni,[27] A.Engler,[37] F.J.Eppling,[17] F.C.Erné,[2] J.P.Ernenwein,[27] P.Extermann,[21] M.Fabre,[49] R.Faccini,[39] S.Falciano,[39] A.Favara,[18] J.Fay,[27] M.Felcini,[51] C.Furetta,[29] T.Ferguson,[37] D.Fernandez,[28] F.Ferroni,[39] H.Fesefeldt,[1] E.Fiandrini,[36] J.H.Field,[21] F.Filthaut,[37] P.H.Fisher,[17] G.Forconi,[17] L.Fredj,[21] K.Freudenreich,[51] Yu.Galaktionov,[30,17] S.N.Ganguli,[11] S.S.Gau,[13] S.Gentile,[39] J.Gerald,[5] N.Gheordanescu,[14] S.Giagu,[39] S.Goldfarb,[24] J.Goldstein,[12] Z.F.Gong,[22] A.Gougas,[5] G.Gratta,[35] M.W.Gruenewald,[9] V.K.Gupta,[38] A.Gurtu,[11] L.J.Gutay,[48] K.Hangarter,[1] B.Hartmann,[1] A.Hasan,[32] T.Hebbeker,[9] A.Hervé,[19] W.C.van Hoek,[33] H.Hofer,[51] H.Hoorani,[21] S.R.Hou,[53] G.Hu,[20] M.M.Ilyas,[20] V.Innocente,[19] H.Janssen,[4] B.N.Jin,[8] L.W.Jones,[3] P.de Jong,[17] I.Josa-Mutuberria,[28] A.Kasser,[24] R.A.Khan,[20] Yu.Kamyshkov,[34] P.Kapinos,[50] J.S.Kapustinsky,[26] Y.Karyotakis,[4] M.Kaur,[20,♢] M.N.Kienzle-Focacci,[21] D.Kim,[5] J.K.Kim,[45] S.C.Kim,[45] Y.G.Kim,[45] W.W.Kinnison,[26] A.Kirkby,[35] D.Kirkby,[35] J.Kirkby,[19] W.Kittel,[33] A.Klimentov,[17,30] A.C.König,[33] A.Köngeter,[1] I.Korolko,[30] V.Koutsenko,[17,30] A.Koulbardis,[40] R.W.Kraemer,[37] T.Kramer,[17] W.Krenz,[1] H.Kuijten,[33] A.Kunin,[17,30] P.Ladron de Guevara,[28] G.Landi,[18] C.Lapoint,[17] K.Lassila-Perini,[51] M.Lebeau,[19] A.Lebedev,[17] P.Lebrun,[27] P.Lecomte,[51] P.Lecoq,[19] P.Le Coultre,[51] J.S.Lee,[45] K.Y.Lee,[45] J.M.Le Goff,[19] R.Leiste,[50] M.Lenti,[18] E.Leonardi,[39] P.Levtchenko,[40] C.Li,[22] E.Lieb,[50] W.T.Lin,[53] F.L.Linde,[2,19] B.Lindemann,[1] L.Lista,[31] Z.A.Liu,[8] W.Lohmann,[50] E.Longo,[39] W.Lu,[35] Y.S.Lu,[8] K.Lübelsmeyer,[1] C.Luci,[39] D.Luckey,[17] L.Ludovici,[39] L.Luminari,[39] W.Lustermann,[49] W.G.Ma,[22] A.Macchiolo,[18] M.Maity,[11] G.Majumder,[11] L.Malgeri,[39] A.Malinin,[30] C.Maña,[28] S.Mangla,[11] P.Marchesini,[51] A.Marin,[12] J.P.Martin,[27] F.Marzano,[39] G.G.G.Massaro,[2] K.Mazumdar,[11] D.McNally,[19] R.R.McNeil,[7] S.Mele,[31] L.Merola,[31] M.Meschini,[18] W.J.Metzger,[33] M.von der Mey,[1] Y.Mi,[24] A.Mihul,[14] A.J.W.van Mil,[33] G.Mirabelli,[39] J.Mnich,[19] M.Möller,[1] B.Monteleoni,[18] R.Moore,[3] S.Morganti,[39] R.Mount,[35] S.Müller,[1] F.Muheim,[21] E.Nagy,[15] S.Nahn,[17] M.Napolitano,[31] F.Nessi-Tedaldi,[51] H.Newman,[35] A.Nippe,[1] H.Nowak,[50] G.Organtini,[39] R.Ostonen,[23] D.Pandoulas,[1] S.Paoletti,[39] P.Paolucci,[31] H.K.Park,[37] G.Pascale,[39] G.Passaleva,[18] S.Patricelli,[31] T.Paul,[36] M.Pauluzzi,[36] C.Paus,[1] F.Pauss,[51] D.Peach,[19] Y.J.Pei,[1] S.Pensotti,[29] D.Perret-Gallix,[4] S.Petrak,[9] A.Pevsner,[5] D.Piccolo,[31] M.Pieri,[18] J.C.Pinto,[37] P.A.Piroué,[38] E.Pistolesi,[18] V.Plyaskin,[30] M.Pohl,[51] V.Pojidaev,[30,18] H.Postema,[17] N.Produit,[21] R.Raghavan,[11] G.Rahal-Callot,[51] P.G.Rancoita,[29] M.Rattaggi,[29] G.Raven,[42] P.Razis,[32] K.Read,[34] D.Ren,[51] M.Rescigno,[39] S.Reucroft,[13] T.van Rhee,[47] A.Ricker,[1] S.Riemann,[50] B.C.Riemers,[48] K.Riles,[3] S.Ro,[45] A.Robohm,[51] J.Rodin,[17] F.J.Rodriguez,[28] B.P.Roe,[3] S.Röhner,[1] L.Romero,[28] S.Rosier-Lees,[4] Ph.Rosselet,[24] W.van Rossum,[47] S.Roth,[1] J.A.Rubio,[19] H.Rykaczewski,[51] J.Salicio,[19] E.Sanchez,[28] A.Santocchia,[36] M.E.Sarakinos,[23] S.Sarkar,[11] M.Sassowsky,[1] C.Schäfer,[1] V.Schegelsky,[40] S.Schmidt-Kaerst,[1] D.Schmitz,[1] P.Schmitz,[1] M.Schneegans,[4] B.Schoeneich,[50] N.Scholz,[51] H.Schopper,[52] D.J.Schotanus,[33] R.Schulte,[1] K.Schultze,[1] J.Schwenke,[1] G.Schwering,[1] C.Sciacca,[31] D.Sciarrino,[21] J.C.Sens,[53] L.Servoli,[36] S.Shevchenko,[35] N.Shivarov,[44] V.Shoutko,[30] J.Shukla,[26] E.Shumilov,[30] T.Siedenburg,[1] D.Son,[45] A.Sopczak,[50] B.Smith,[17] P.Spillantini,[18] M.Steuer,[17] D.P.Stickland,[38] F.Sticozzi,[17] H.Stone,[38] B.Stoyanov,[44] A.Straessner,[1] K.Strauch,[16] K.Sudhakar,[11] G.Sultanov,[20] L.Z.Sun,[22] G.F.Susinno,[21] H.Suter,[51] J.D.Swain,[20] X.W.Tang,[8] L.Tauscher,[6] L.Taylor,[13] Samuel C.C.Ting,[17] S.M.Ting,[17] O.Toker,[36] F.Tonisch,[50] M.Tonutti,[1] S.C.Tonwar,[11] J.Tóth,[15] A.Tsaregorodtsev,[40] C.Tully,[38] H.Tuchscherer,[46] K.L.Tung,[8] J.Ulbricht,[51] U.Uwer,[19] E.Valente,[39] R.T.Van de Walle,[33] I.Vetlitsky,[30] G.Viertel,[51] M.Vivargent,[4] R.Völkert,[50] H.Vogel,[37] H.Vogt,[50] I.Vorobiev,[30] A.A.Vorobyov,[40] An.A.Vorobyov,[40] A.Vorvolakos,[32] M.Wadhwa,[6] W.Wallraff,[1] J.C.Wang,[17] X.L.Wang,[22] Y.F.Wang,[17] Z.M.Wang,[22] A.Weber,[1] F.Wittgenstein,[19] S.X.Wu,[20] S.Wynhoff,[1] J.Xu,[12] Z.Z.Xu,[22] B.Z.Yang,[22] C.G.Yang,[8] X.Y.Yao,[8] J.B.Ye,[22] S.C.Yeh,[53] J.M.You,[37] C.Zaccardelli,[35] An.Zalite,[40] P.Zemp,[51] Y.Zeng,[1] Z.Zhang,[8] Z.P.Zhang,[22] B.Zhou,[12] Y.Zhou,[3] G.Y.Zhu,[8] R.Y.Zhu,[35] A.Zichichi.[10,19,20]

1 I. Physikalisches Institut, RWTH, D-52056 Aachen, FRG[§]
III. Physikalisches Institut, RWTH, D-52056 Aachen, FRG[§]
2 National Institute for High Energy Physics, NIKHEF, and University of Amsterdam, NL-1009 DB Amsterdam, The Netherlands
3 University of Michigan, Ann Arbor, MI 48109, USA
4 Laboratoire d'Annecy-le-Vieux de Physique des Particules, LAPP,IN2P3-CNRS, BP 110, F-74941 Annecy-le-Vieux CEDEX, France
5 Johns Hopkins University, Baltimore, MD 21218, USA
6 Institute of Physics, University of Basel, CH-4056 Basel, Switzerland
7 Louisiana State University, Baton Rouge, LA 70803, USA
8 Institute of High Energy Physics, IHEP, 100039 Beijing, China
9 Humboldt University, D-10099 Berlin, FRG[§]
10 INFN-Sezione di Bologna, I-40126 Bologna, Italy
11 Tata Institute of Fundamental Research, Bombay 400 005, India
12 Boston University, Boston, MA 02215, USA
13 Northeastern University, Boston, MA 02115, USA
14 Institute of Atomic Physics and University of Bucharest, R-76900 Bucharest, Romania
15 Central Research Institute for Physics of the Hungarian Academy of Sciences, H-1525 Budapest 114, Hungary[‡]
16 Harvard University, Cambridge, MA 02139, USA
17 Massachusetts Institute of Technology, Cambridge, MA 02139, USA
18 INFN Sezione di Firenze and University of Florence, I-50125 Florence, Italy
19 European Laboratory for Particle Physics, CERN, CH-1211 Geneva 23, Switzerland
20 World Laboratory, FBLJA Project, CH-1211 Geneva 23, Switzerland
21 University of Geneva, CH-1211 Geneva 4, Switzerland
22 Chinese University of Science and Technology, USTC, Hefei, Anhui 230 029, China
23 SEFT, Research Institute for High Energy Physics, P.O. Box 9, SF-00014 Helsinki, Finland
24 University of Lausanne, CH-1015 Lausanne, Switzerland
25 INFN-Sezione di Lecce and Universitá Degli Studi di Lecce, I-73100 Lecce, Italy
26 Los Alamos National Laboratory, Los Alamos, NM 87544, USA
27 Institut de Physique Nucléaire de Lyon, IN2P3-CNRS,Université Claude Bernard, F-69622 Villeurbanne, France
28 Centro de Investigaciones Energeticas, Medioambientales y Tecnologicas, CIEMAT, E-28040 Madrid, Spain[♭]
29 INFN-Sezione di Milano, I-20133 Milan, Italy
30 Institute of Theoretical and Experimental Physics, ITEP, Moscow, Russia
31 INFN-Sezione di Napoli and University of Naples, I-80125 Naples, Italy
32 Department of Natural Sciences, University of Cyprus, Nicosia, Cyprus
33 University of Nymegen and NIKHEF, NL-6525 ED Nymegen, The Netherlands
34 Oak Ridge National Laboratory, Oak Ridge, TN 37831, USA
35 California Institute of Technology, Pasadena, CA 91125, USA
36 INFN-Sezione di Perugia and Universitá Degli Studi di Perugia, I-06100 Perugia, Italy
37 Carnegie Mellon University, Pittsburgh, PA 15213, USA
38 Princeton University, Princeton, NJ 08544, USA
39 INFN-Sezione di Roma and University of Rome, "La Sapienza", I-00185 Rome, Italy
40 Nuclear Physics Institute, St. Petersburg, Russia
41 University and INFN, Salerno, I-84100 Salerno, Italy
42 University of California, San Diego, CA 92093, USA
43 Dept. de Fisica de Particulas Elementales, Univ. de Santiago, E-15706 Santiago de Compostela, Spain
44 Bulgarian Academy of Sciences, Central Laboratory of Mechatronics and Instrumentation, BU-1113 Sofia, Bulgaria
45 Center for High Energy Physics, Korea Advanced Inst. of Sciences and Technology, 305-701 Taejon, Republic of Korea
46 University of Alabama, Tuscaloosa, AL 35486, USA
47 Utrecht University and NIKHEF, NL-3584 CB Utrecht, The Netherlands
48 Purdue University, West Lafayette, IN 47907, USA
49 Paul Scherrer Institut, PSI, CH-5232 Villigen, Switzerland
50 DESY-Institut für Hochenergiephysik, D-15738 Zeuthen, FRG
51 Eidgenössische Technische Hochschule, ETH Zürich, CH-8093 Zürich, Switzerland
52 University of Hamburg, D-22761 Hamburg, FRG
53 High Energy Physics Group, Taiwan, China
Supported by the German Bundesministerium für Bildung, Wissenschaft, Forschung und Technologie
Supported by the Hungarian OTKA fund under contract number T14459.
♭ Supported also by the Comisión Interministerial de Ciencia y Tecnología
♯ Also supported by CONICET and Universidad Nacional de La Plata, CC 67, 1900 La Plata, Argentina
♢ Also supported by Panjab University, Chandigarh-160014, India

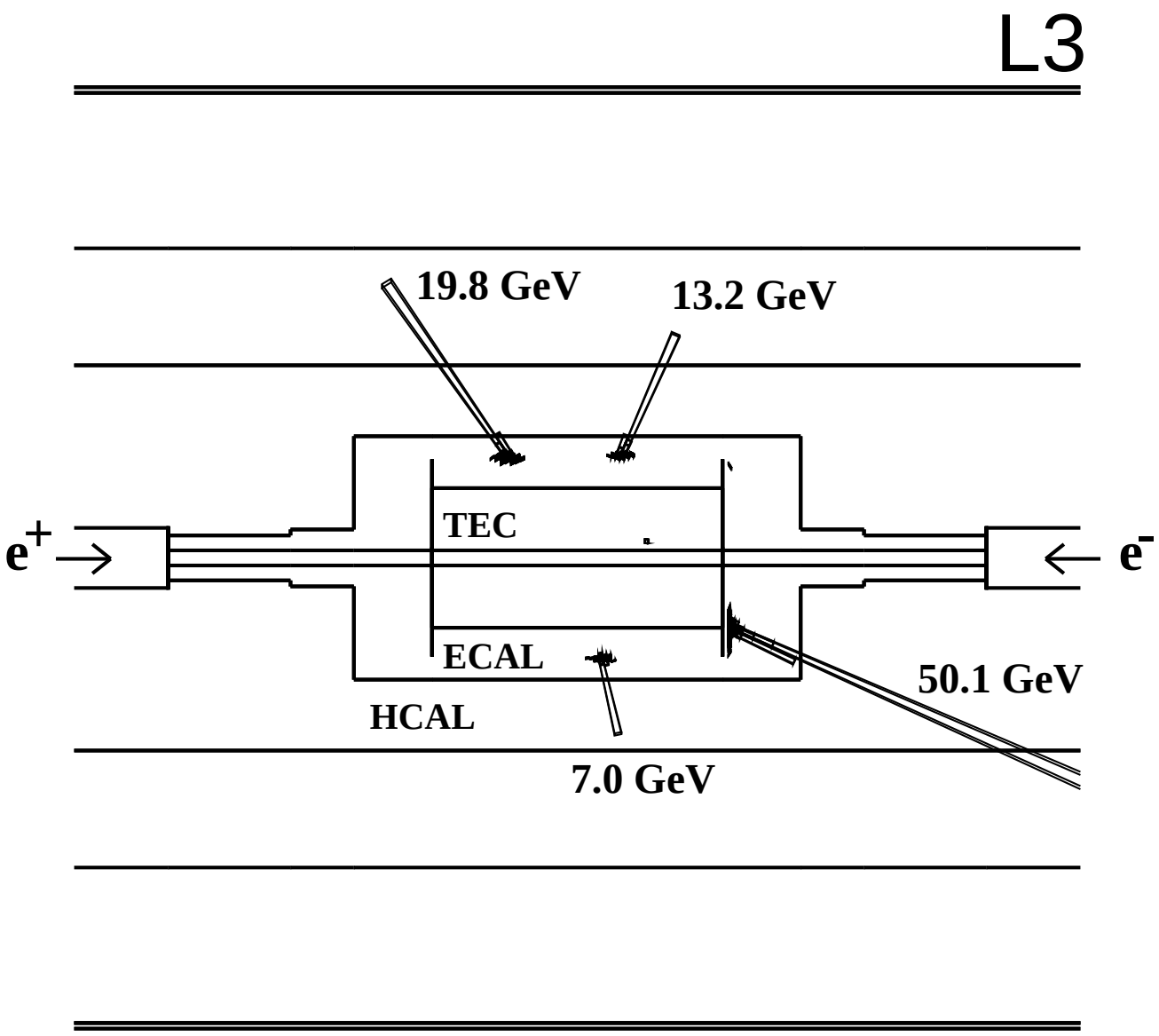

Figure 1: Longitudinal view of the event with four isolated photons recorded by the L3 detector at a center-of-mass energy of 130 GeV. Energy depositions in the ECAL are shown as a polar histogram. There are no hits in the central tracking detector indicating the presence of charged particles. The event has a longitudinal energy imbalance consistent with the production of an unobserved photon of 40 GeV at very low polar angle.

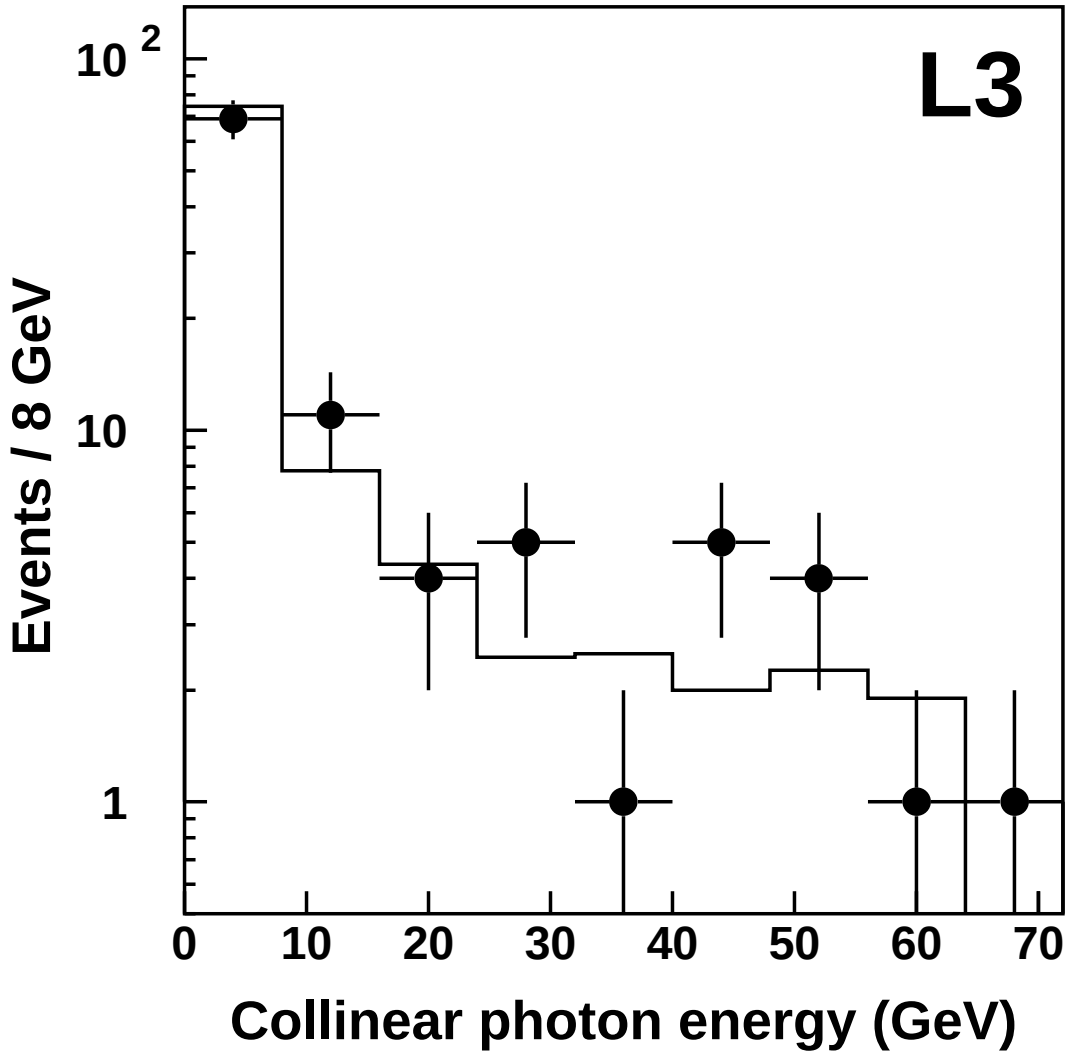

Figure 2: Energy spectrum of collinear photons in the $\gamma\gamma(\gamma)$ sample at a mean center-of-mass energy of 133 GeV, compared to the Monte Carlo prediction. The energy of the collinear photon has been determined from the invariant mass of the two most energetic photons, under the assumption that there is one zero mass missing particle.

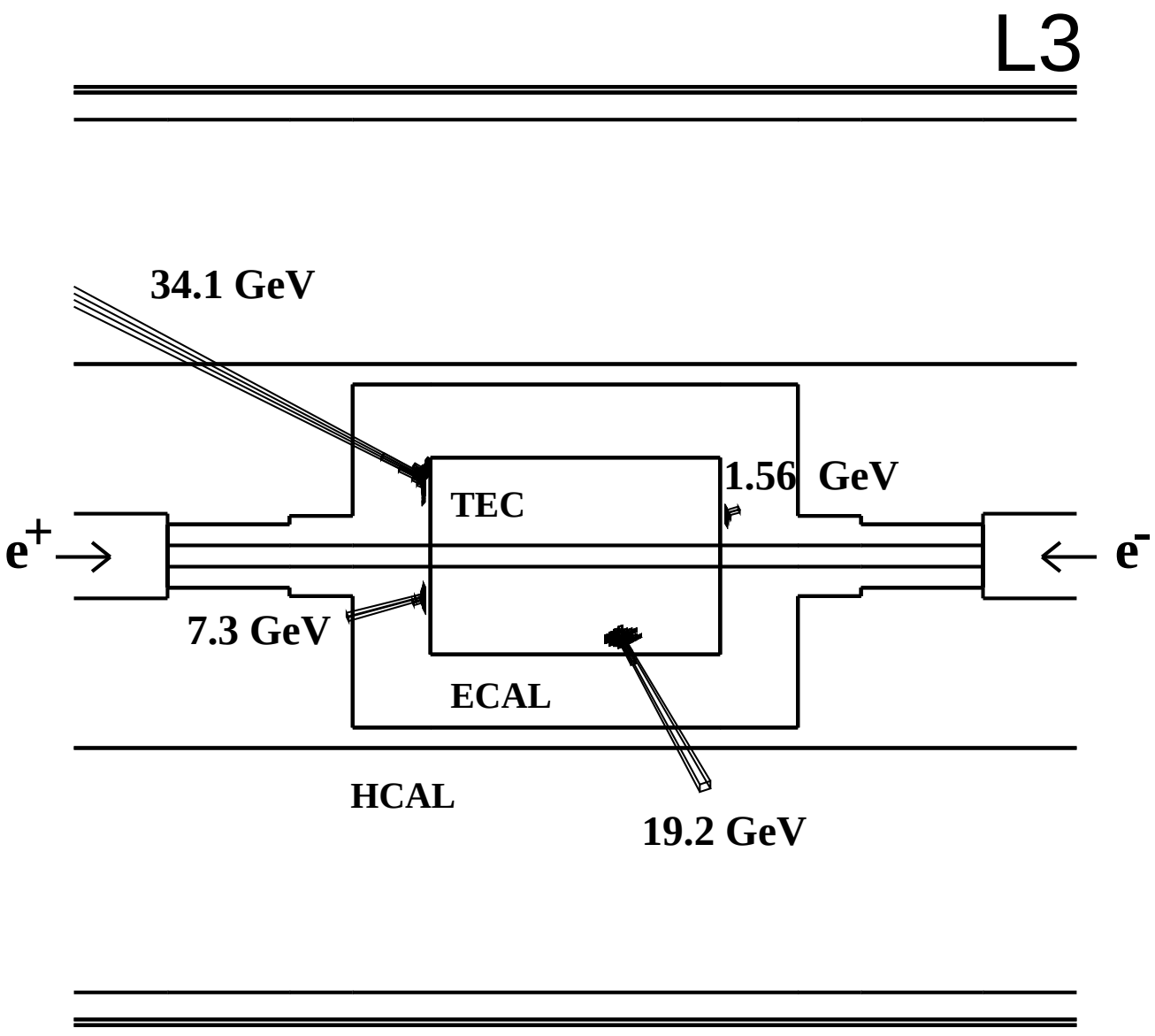

Figure 3: Longitudinal view of the event with four isolated photons recorded by the L3 detector at LEP1. The center-of-mass energy of the collision is 89.5 GeV. Energy depositions in the ECAL are shown as a polar histogram. There are no hits in the central tracking detector indicating the presence of charged particles. The event has a longitudinal energy imbalance consistent with the production of an unobserved photon of 27 GeV at very low polar angle.

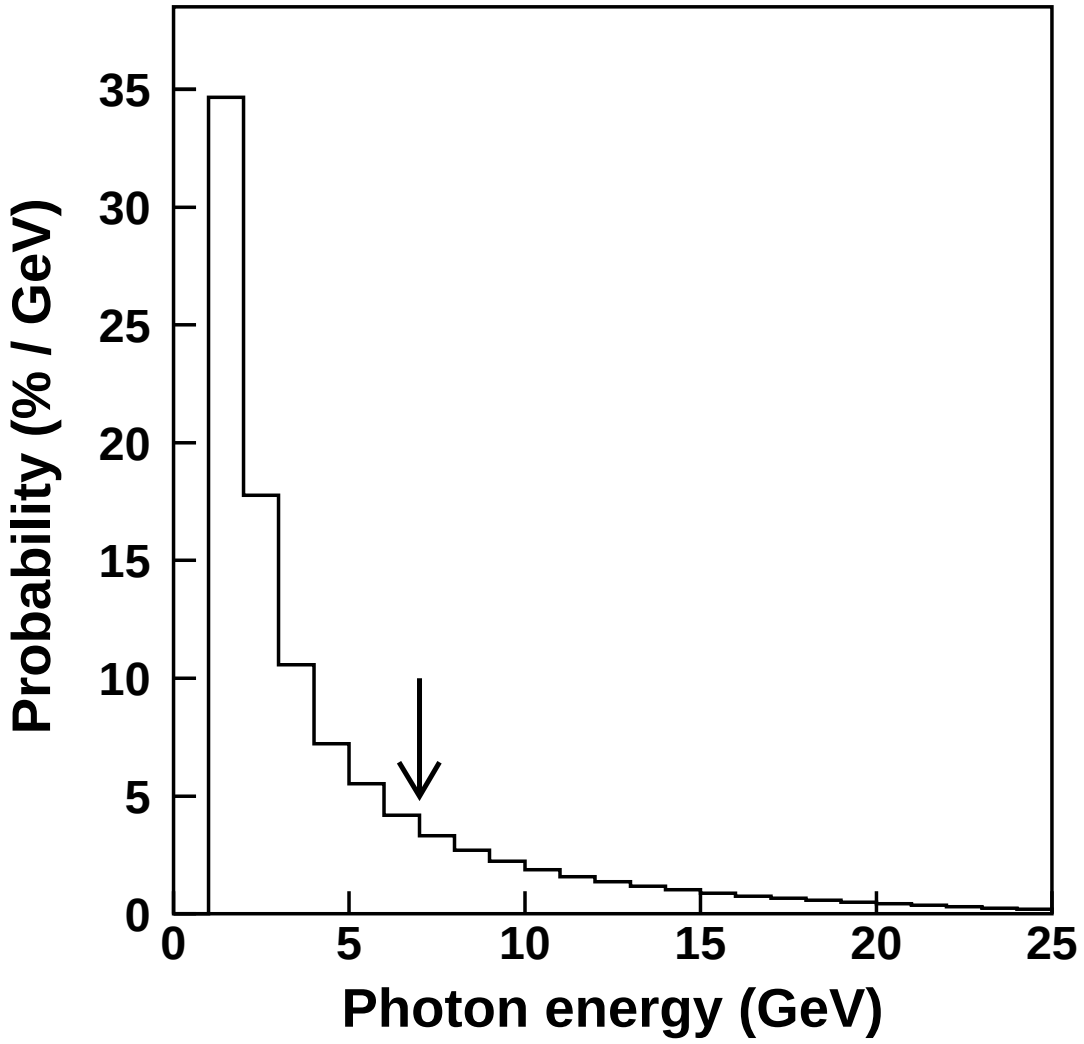

Figure 4: Differential probability as a function of the energy of the least energetic photon in Monte Carlo $\gamma\gamma\gamma\gamma$ events. The histogram is the tree-level generator prediction after all energy and angular cuts have been applied. The arrow shows the position of the $\gamma\gamma\gamma\gamma(\gamma)$ event found in the L3 sample.

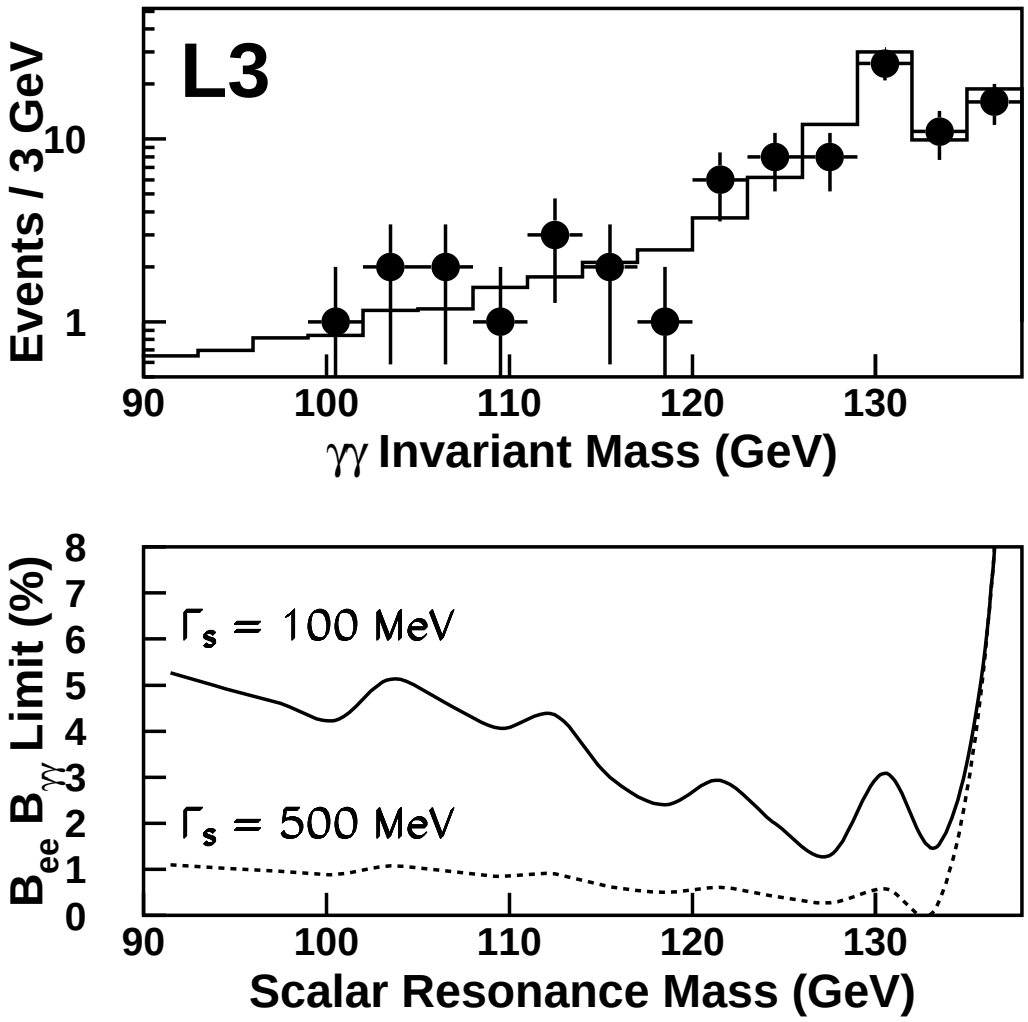

Figure 5: Invariant-mass spectrum of the two most energetic photons in $\gamma\gamma(\gamma)$ events and limits on the existence of a narrow scalar resonance coupled to electrons and photons. The bin size (3 GeV) is approximately twice the expected invariant mass resolution. We determine upper limits (at the 95 % CL) on the product $B_{ee}B_{\gamma\gamma}$, where B_{ee} is the branching ratio of the scalar resonance into electrons pairs and $B_{\gamma\gamma}$ its branching ratio into photon pairs. Two cases for the scalar resonance width, $\Gamma_S = 100$ MeV and $\Gamma_S = 500$ MeV, are shown.

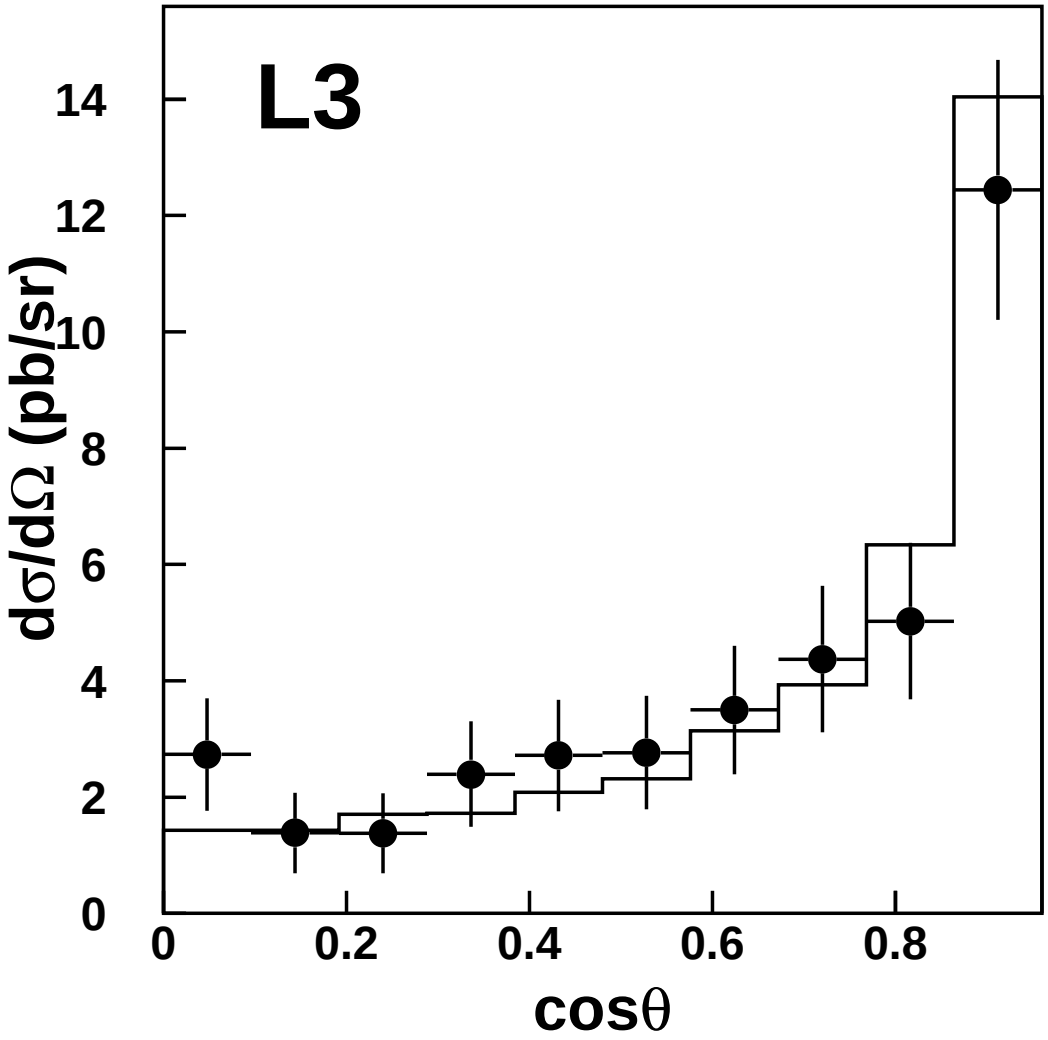

Figure 6: Differential cross section as a function of the polar angle for $\gamma\gamma(\gamma)$ events. The points are data at an average center-of-mass energy of 133 GeV. The histogram is the Monte Carlo simulation of the $e^+e^- \to \gamma\gamma(\gamma)$ process.

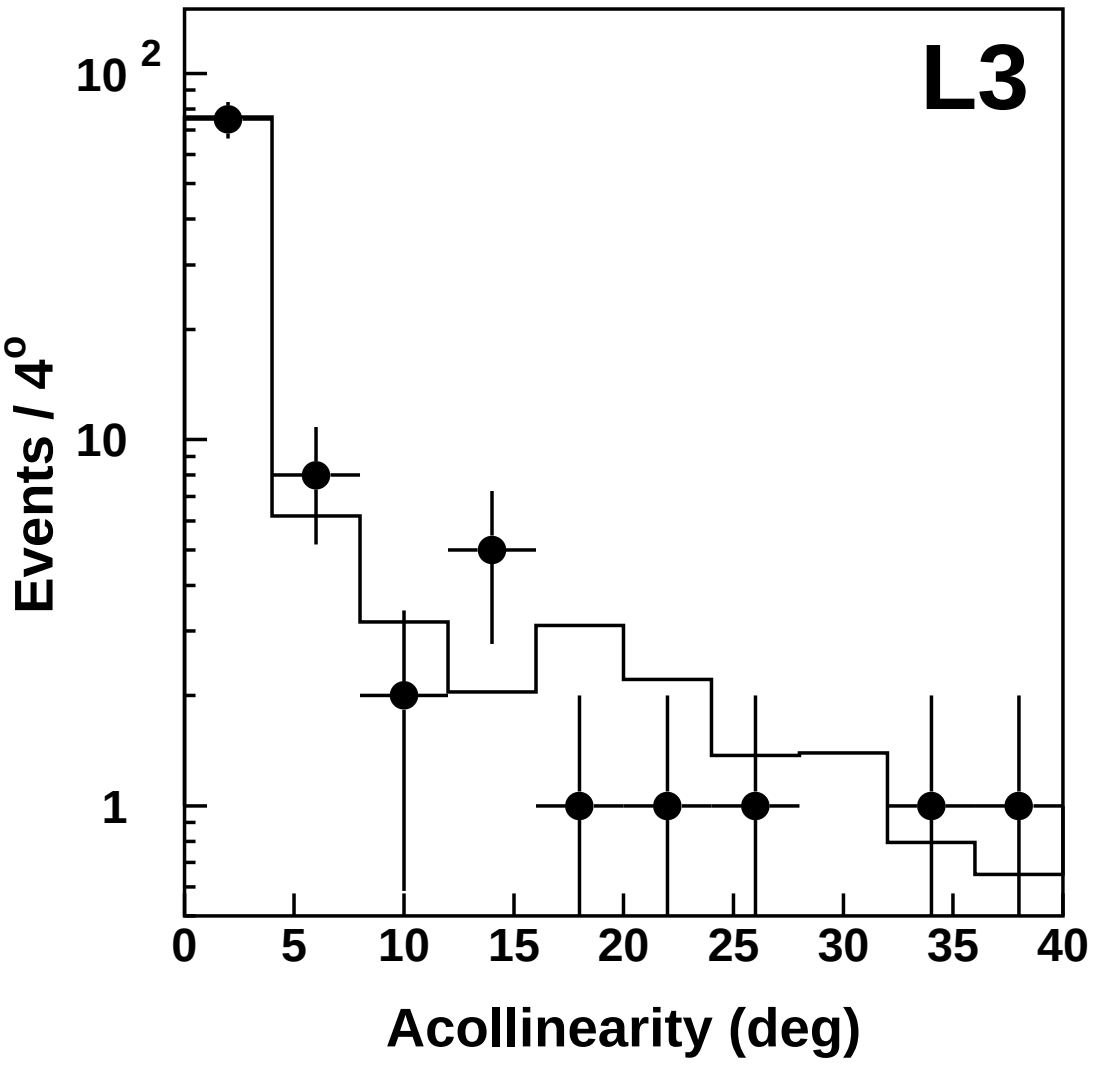

Figure 7: Distribution of the acollinearity between the two most energetic photons in the $e^+e^- \to \gamma\gamma(\gamma)$ process at an average center-of-mass energy of 133 GeV. The points are data and the histogram is Monte Carlo.